STABILIZATION OF FREE RADICAL INTERMEDIATES
ON METAL OXIDE SEMICONDUCTOR SURFACES

Detlef W. Bahnemann and Michael R. Hoffmann

Bereich Strahlenchemie, Hahn-Meitner-Institut GmbH,
Glienicker Str. 100, D-1000 Berlin 39,
Germany
and
W. M. Keck Laboratories, California Institute of
Technology, 1201 California Blvd., Pasadena, CA 91125,
USA

Abstract

Free radicals intermediates are formed on the surface
of metal oxide semiconductors, namely TiO_2 and Fe_2O_3,
following the light-induced charge separation upon
band-gap illu-mination. These radicals appear to adhe-
re strongly to the surfaces of the small colloidal
particles (diameters between 5 and 20 nm) employed in
this study. A second electron-transfer step yielding
the observed end-products therefore preceeds desorp-
tion of the reactive intermediates. Oxidation of me-
thylviologen (1,1'-dimethyl-4,4'bipyridylium chloride)
and reduction of halothane (2-bromo-2-chloro-1,1,1-
trifluoroethane) is thus found to proceed with high
quantum yields and very specific mechanisms on colloi-
dal TiO_2. The oxidation of sulfite on α-Fe_2O_3 partic-
les yields the sulfite radical anion, $SO_3^{\cdot-}$, as
initial intermediate. A subsequent electron transfer
leading to the formation of sulfate occurs on the sur-
face of the same catalyst particle.

Introduction

A wide variety of chemical reactions can be photocatalyzed
employing suspensions of semiconductor particles under band-gap
illumination (1 - 3). While the overall stoichiometry of many
such organic and inorganic conversions has been studied extensive-
ly (4 - 6), not much emphasis has been put on the understanding
of mechanistic details. This paper focusses on the fate of free
radical intermediates photo-generated on the surface of TiO_2 and
α-Fe_2O_3 particles. The use of transparent colloidal suspensions
of these materials enabled us to determine quantum yields of all
products. Furthermore, spectroscopic studies could be carried out
like in homogenous solution since light-scattering did not pose a
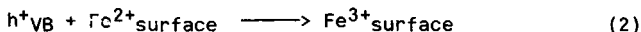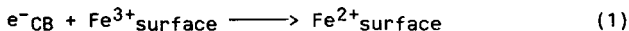problem under the experimental conditions.

Experimental

The preparation of optically transparent aqueous suspensions of TiO_2 has been described (7). If necessary photoplatinization of the tiny colloidal particles (5 nm $\leqslant$ d $\leqslant$ 20 nm) was achieved by illumination (λ_{ex} = 366 nm) of these suspensions in the presence of 10^{-4} M H_2PtCl_6 and 0.1 M CH_3OH. Small colloidal hematite particles were obtained by the dropwise addition of 150 ml of a freshly prepared aqueous solution of $FeCl_3$ (0.1 M) to 1350 ml of vigorously boiling water followed by a continuous hydrolysis at 100 °C for 50h. The resulting clear colloidal suspension could be dialyzed to neutrality and contained hexagonal platelets of α-Fe_2O_3 with sizes between 5 and 20 nm. Reaction products were analyzed with HPIC, TLC or GC, the sulfite concentration was determined using a colorimetric method (8). Monochromatic light was employed in all photolysis experiments, experimental set-up and actinometry have been described (9,10).

Results and Discussion

Two strongly fluorescing oxidation products have recently been identified when methylviologen (MV^{2+}) reacts with OH$^{\cdot}$ radicals in aqueous solution. However, these compounds, namely the 1',2'-dihydro-1,1'-dimethyl-2'-oxo-4,4'-bipyridylium cation ('2-one') and the 3,4-dihydro-1,1'dimethyl-3-oxo-4,4'-bipyridylium cation ('3-one'), are only formed as side-products in an overall very complex reaction mixture (11). Figure 1 shows the quantum yield of the photocatalytic formation of 2-one and 3-one upon band-gap illumination (1mM hν with λ_{ex} = 366 nm) of aerated aqueous colloidal TiO_2 solutions (0.5g/ℓ) containing 5mM MV^{2+} at pH 11.5. Together both products are formed with a comparatively high quantum yield: Φ = 0.042. Thus a mechanism is suggested to explain the specificity of TiO_2 for methylviologen oxidation (Fig. 2). Photogenerated valence band holes (h^+_{VB}) initially form adsorbed OH$^{\cdot}$ radicals which react with MV^{2+} yielding MV(-H)-OH$^{\cdot+}$ radical cations. Diffusion of the latter into the bulk solution should result in a product distribution similar to that in homogenous solution and therefore only small yields of fluorescing products. Hence it is reasonable to assume that the radical cations remain on the negatively charged particle's surface until further oxidation by another hole (formed via absorption of a subsequent photon by the same oxide particle) leads to the observed products. As shown in Fig. 2, MV^{2+} simultanously acts as electron scavenger suppressing the electron/hole recombination. No attempts were made in this study to further investigate this reductive path. Based on the proposed mechanism it is calculated that 8.4 % of all absorbed photons lead to the formation of one of the two fluorescing oxidation products.

It is interesting to note the effect of ferric ions on the yield of the keto species (Fig. 1). While addition of Fe^{3+} clearly enhanced the formation of 2-one and 3-one in the radiation chemical experiments (11), it strongly suppresses their production in the photocatalytic system. This inhibitory effect can be rationalized in terms of a 'short-circuiting' of the catalyst via

$$e^-_{CB} + Fe^{3+}_{surface} \longrightarrow Fe^{2+}_{surface} \qquad (1)$$

$$h^+_{VB} + Fe^{2+}_{surface} \longrightarrow Fe^{3+}_{surface} \qquad (2)$$

It has recently been shown that the one-electron reduction of halothane in homogenous aqueous solution leads to the formation of bromide ions and a carbon-centered radical (12):

$$e^-_{aq} + CF_3CHBrCl \longrightarrow CF_3CHCl^{\cdot} + Br^- \qquad (3)$$
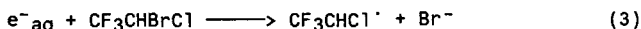
In the presence of molecular oxygen the latter is readily converted into the corresponding peroxy-radical and subsequently into trifluoroacetate (TFA^-) and other products. If, however, under anoxic conditions another reductant such as ascorbate is present, the formation of fluoride ions follows:
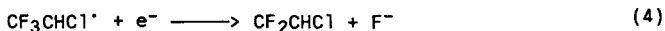
$$CF_3CHCl^{\cdot} + e^- \longrightarrow CF_2CHCl + F^- \qquad (4)$$

Fig. 3 shows the ionic products observed upon band-gap illumination (2 μM hν/s with λ_{ex} = 366 nm) of photoplatinized TiO_2 (0.5g/ℓ, pH 11.5) in the presence of 10mM halothane, 1M methanol and air. It is apparent that both, fluoride and bromide ions are formed in high concentrations while TFA^- is only seen in minute amounts. Note, that no F^- could be detected when halothane is reduced by e^-_{aq} in homogenous solution under otherwise identical conditions even in the presence of additional reductants. Quantum yields of ϕ = 0.43 are calculated for the formation of F^- and Br^- from the curves in Fig. 3 just illustrating the remarkable efficiency of the catalyst. The suggested reaction mechanism is shown in Fig. 4. The initial reduction of halothane by e^-_{CB} leads to the formation of Br^- and the $CF_3CHCl^{\cdot}$ radical (methanol acts as hole scavenger in these experiments). From the high yields of F^- production it is inferred that the radical remains on the surface of the same particle to accept another conduction band electron. Alternatively, it is feasible that $CF_3CHCl^{\cdot}$ reacts with $^{\cdot}CH_2OH$ via

$$CF_3CHCl^{\cdot} + {}^{\cdot}CH_2OH \longrightarrow CF_2CHCl + CH_2O + HF \qquad (5)$$
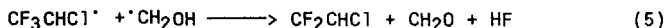
yielding the same products. However, also this reaction should occur on that surface where the radicals were originally generated, since a detailed study evinced the absence of free radical reactions in the bulk of the solution (12).

This adsorption phenomenum of free radical intermediates is apparently not restricted to titanium dioxide surfaces. Fig. 5 shows the rapid oxidation of sulfite ions with α-Fe_2O_3 particles being the active photocatalysts. The intermediate formation of $SO_3^{\cdot-}$ radicals is deduced from the detection of $S_2O_6^{2-}$ as another reaction product besides SO_4^{2-} when O_2 is excluded (sulfate is the only product in aerated suspensions). The finding that the quantum yield of sulfite oxidation (calculated from the initial slopes in Fig. 5) does not depend on the presence of O_2 (Pt^{4+} acts as the electron acceptor under anoxic conditions) and does not exceed unity, strongly indicates the absence of the typical behavior of freely diffusing $SO_3^{\cdot-}$ radical anions. Chain reactions with chain lengths in the order of 10,000 which have been reported when $SO_3^{\cdot-}$ radicals are generated in solution (13) are certainly not indicated in these colloidal suspensions of α-Fe_2O_3. As shown in Fig. 6, this chain reaction is initiated by the formation of $SO_5^{\cdot-}$ through the reaction of molecular oxygen with $SO_3^{\cdot-}$. Apparently, such a process is of negligable importance in the heterogenous system employed in this study. The observed wavelength dependence of the quantum yield of sulfite oxidation (Fig. 7) clearly shows that hematite indeed acts as the photocatalyst in this system (bandgap of α-$Fe_2O_3 \approx 2.3$ eV or 540 nm, i.e. onset of catalytic activity). The pronounced increase of Φ towards shorter wavelengths is explained by amorphous material still present after the described preparation of the catalyst. Recently it has been shown that amorphous Fe_2O_3 only exhibits photocatalytic activity when illuminated with light below 400 nm (14).

A mechanistic sketch exhibited in Fig. 8 illustrates the envisaged reaction mechanism with an electron transfer occurring on the particle's surface from semi-oxidized S(V) species to adjacent O_2 molecules. Thermodynamic considerations reveal that $SO_3^{\cdot-}$ radical anions should indeed be capable of reducing O_2. With the one-electron oxidation potential E_7^1 ($SO_3^{2-}/SO_3^{\cdot-}$) = 0,84 V vs. NHE (15) and an overall potential E°(SO_3^{2-}/SO_4^{2-}) = 0,11 V vs.NHE a one-electron reduction potential of E_7^1($SO_3^{\cdot-}/SO_4^{2-}$) = -0,62 V vs.NHE is calculated. This is sufficient to reduce molecular oxygen (E_7^1($O_2^{\cdot-}/O_2$) = - 0.33 V vs.NHE (16)). Bond formation yielding $SO_5^{\cdot-}$ radical anions appears to govern the reaction path in homogenous solution leading to the observed reaction chain. On the other hand, specific surface adsorption and compartementalization seem to be the most important criteria deciding upon the reaction sequence in the heterogenous system!

Acknowledgement

References

(1) J. O'M. Bockris, B. Dandapani, D. Cooke, and J. Ghoroghchian, Int. J. Hydrogen Energy 10, 179 (1985).

(2) J. H. Fendler, J. Phys. Chem. 89, 2730 (1985).

(3) G. A. Somorjai, M. Hendewerk, and J. E. Turner, Catal. Rev.-Sci. Eng. 26, 683 (1984).

(4) W. W. Dunn, Y. Aikawa, and A. J. Bard, J. Am. Chem. Soc. 103, 6893 (1981) and refs. cited.

(5) M. A. Fox, Acc. Chem. Res. 16, 314 (1983) and refs. cited therein.

(6) D. F. Ollis, Environ. Sci. Technol. 19, 480 (1985) and refs. cited therein.

(7) D. Bahnemann, A. Henglein, J. Lilie, and L. Spanhel, J. Phys. Chem. 88, 709 (1984).

(8) R. C. Humphrey, M. H. Ward, and W. Hinze, Anal. Chem. 42, 698 (1970).

(9) B. C. Faust and M. R. Hoffmann, Environ. Sci. Technol. 20, 943 (1986).

(10) H. G. Heller and J. R. Langan, J. Chem. Soc., Perkin Trans. 2, 341 (1981).

(11) D. W. Bahnemann, Ch.-H. Fischer, E. Janata and A. Henglein, J. Chem. Soc., Faraday Trans. 1, 83, 2559 (1987).

(12) D. W. Bahnemann, J. Mönig, and R. Chapman, J. Phys. Chem. 91, 3782 (1987) and refs. cited therein.

(13) E. Hayon, E. Treinin, and J. Wilf, J. Am. Chem. Soc. 94, 47 (1972).

(14) D. W. Bahnemann and M. R. Hoffmann, unpublished results.

(15) R. E. Huie and P. Neta, J. Phys. Chem. 88, 5665 (1984).

(16) B. H. J. Bielski, D. E. Cabelli, R. L. Arudi, and A. B. Ross, J. Phys. Chem. Ref. Data 14, 1041 (1985).
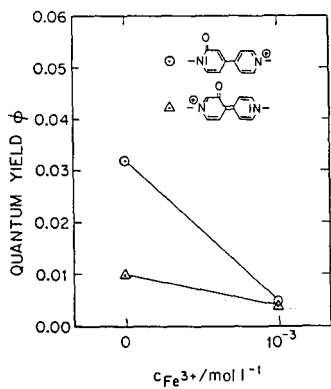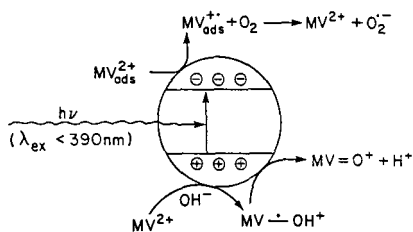
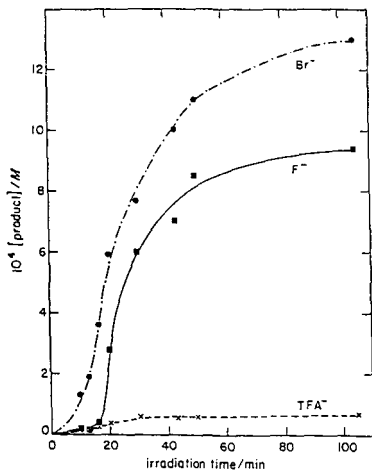Figure 1

TWO ELECTRON OXIDATION OF METHYLVIOLOGEN

Figure 2

Figure 3

TWO ELECTRON TRANSFER TO HALOTHANE
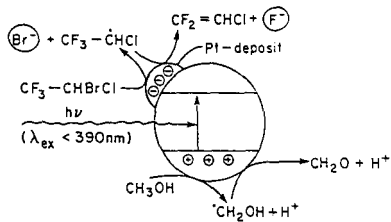
Figure 4

Photooxidation of SO_3^{2-} on colloidal Fe_2O_3

(10^{-4} moles dm^{-3} Fe_2O_3, pH6.9, λ_{ex} = 320nm)

air

10^{-4} moles dm^{-3} Pt^{4+}, N_2
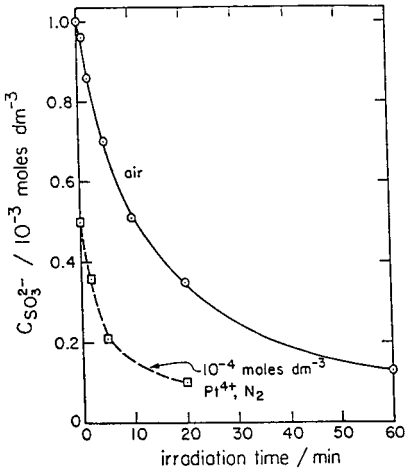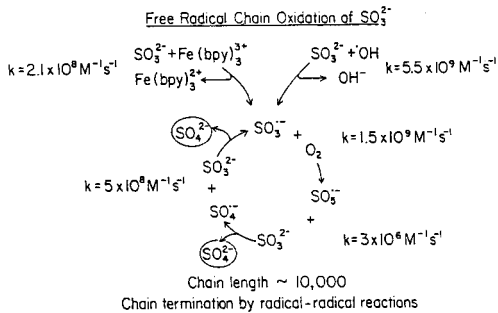
Figure 5

Photooxidation of SO_3^{2-} on colloidal Fe_2O_3

(10^{-3} moles dm^{-3} SO_3^{2-}, pH6.9, Air, 30–50% Abs.)

Figure 7

Free Radical Chain Oxidation of SO_3^{2-}

$k = 2.1 \times 10^8 M^{-1}s^{-1}$

$SO_3^{2-} + Fe(bpy)_3^{3+}$
$Fe(bpy)_3^{2+}$

$SO_3^{2-} + \cdot OH$
OH^-
$k = 5.5 \times 10^9 M^{-1}s^{-1}$

SO_4^{2-}

$SO_3^{\cdot-} +$

$k = 1.5 \times 10^9 M^{-1}s^{-1}$

SO_3^{2-}
$+$
O_2

$k = 5 \times 10^8 M^{-1}s^{-1}$

$SO_4^{\cdot-}$
$+$
SO_3^{2-}

$SO_5^{\cdot-}$

SO_4^{2-}

$k = 3 \times 10^6 M^{-1}s^{-1}$

Chain length ~ 10,000
Chain termination by radical-radical reactions

Figure 6

Mechanistic Ideas

e_{CB}^- scavenged by acceptor (e.g. O_2, Pt^{4+})

Competes with desorption and diffusion to bulk

$\rightleftharpoons SO_3 + H_2O$
$\downarrow$
$SO_4^{2-} + 2H_{aq}^+$

Figure 8